Kasetsart J. (Nat. Sci.) 42 : 776 - 783 (2008)

Differential Scanning Calorimetric Studies of Non-isothermal Crystallization of HDPE and HDPE/$CaCO_3$ Composites

Supreya Trivijitkasem[1*], Thanate Sukkamart[2] and Phanom Kadrun[1]

ABSTRACT

Crystallization of high density polyethylene (HDPE) and HDPE/$CaCO_3$ composites (10, 20 and 30% wt, $CaCO_3$) was investigated by differential scanning calorimetry (DSC) under non-isothermal conditions. The Avrami method modified by Jeziorny and a method developed by Liu *et al*. were employed to describe the non-isothermal crystallization process of the samples. The results showed that the Avrami exponent *n* decreased from 3.0 to 2.4 with an increase in the cooling rate from 5°C/min to 40°C/min, while the crystal growth constant Z_c was nearly constant (~1.1) at a 10°C /min – 40°C/min cooling rate for all systems. The value of *F(T)* showed that the crystallization rate of the HDPE/10% $CaCO_3$ composite was the slowest at a given cooling rate. Moreover, the activation energy determined from the Kissinger method indicated little difference in the values of the activation energy for all systems, except the 30% $CaCO_3$ system which showed a slightly higher activation energy.

Key words: non-isothermal crystallization, HDPE, HDPE/$CaCO_3$

INTRODUCTION

High density polyethylene (HDPE) is a polymeric material which is used in a wide range of applications. The synthesis of pure polymeric materials involves high cost and in addition, the products are manufactured to withstand environmental degradation, which leads to an increase in the amount of plastic waste. A common way to reduce the cost of processing and to accelerate the degradation of plastic waste is to include additives in the polymeric matrix.

Characterizing the thermal properties of polymeric materials provides useful information for the processing stage and aids in the prediction of some of the features of the material. Non-isothermal crystallization behavior is one of the thermal properties that can be characterized, because industrial processing techniques are generally carried out under non-isothermal conditions.

Non-isothermal crystallization features of HDPE and its blends with a variety of additives have been extensively carried out by many researchers (Fonseca and Harrison, 1998; Salazar *et al*., 2002; Krumme *et al*., 2004; Zhang *et al*., 2006). Various theoretical methods have been employed to determine the non-isothermal crystallization kinetics. Mehta *et al*. (2004) used a classical Johnson-Mehl-Avrami (JMA) model to investigate the non-isothermal crystallization kinetics of Ag-doped chalcogenide glasses. Wang *et al*. (2006) employed the Jeziorny method derived from Avrami analysis and a method

1 Department of Physics, Faculty of Science, Kasetsart University, Bangkok 10900, Thailand.

2 Demonstration School, Prince of Songkla University, Meaung, Pattani 94000, Thailand.

* Corresponding author, e-mail: fscisum@ku.ac.th

Received date : 28/05/08 Accepted date : 31/07/08

developed by Liu to describe the non-isothermal crystallization process of organic-inorganic hybrid materials. In this work, the melting behavior of typical commercially-available HDPE and HDPE/$CaCO_3$ composites were studied by differential scanning calorimetry (DSC) and the non-isothermal kinetics were analyzed using the Jeziorny model and the Liu model.

MATERIALS AND METHODS

Commercial-grade raw material HDPE/ x $CaCO_3$ (x = 0, 10, 20 and 30% wt) was supplied by Thantawan Industry, Nakhon Pathom. A Perkin-Elmer DSC7 was used to measure the non-isothermal crystallization kinetics in the cooling mode of the molten state. The temperature and energy readings were calibrated with indium. The measurements were carried out in a nitrogen atmosphere with a 20 ml/min flow rate. The samples were weighed and then placed in sealed aluminum crucibles of 50 µl at 30°C for 2 min. The non-isothermal melt crystallization was initiated by rapidly heating first at a rate of 100° C/min to 180°C and then kept at 180°C for 10 min in the crucible to eliminate any previous thermal history. The samples were then cooled at five constant rates of 5, 10, 20, 30 and 40°C/min. The exothermic crystallization was then recorded as a function of temperature.

RESULTS AND DISCUSSION

Crystallization behavior

The typical DSC curves of heat flow as a function of temperature at the five different cooling rates for the HDPE and the HDPE/$CaCO_3$ composites are shown in Figure 1. Table 1 presents, the non-isothermal crystallization parameters determined from the DSC curves; the onset crystallization temperature T_o; the end of crystallization temperature T_e; the exothermic peak temperature T_p; and the crystallization enthalpy ΔH_c. The parameters T_o, T_e and T_p all decreased as the cooling rate increased. It was also evident that the addition of $CaCO_3$ in HDPE did not cause any significant change in the non-isothermal crystallization temperatures. The crystallization enthalpy ΔH_c increased with an increase in the cooling rate and a decrease in the $CaCO_3$ content.

The relative degree of crystallinity $X(T)$ as a function of temperature is defined by equation 1:

$$X(T) = \int_{T_0}^{T} (dH_c / dT)dT \Big/ \int_{T_0}^{T_c} (dH_c / dT)dT \quad \text{Equation 1}$$

where:

dH_c/dT is the heat flow rate.

In the non-isothermal crystallization process, the time t is related to the temperature T and the cooling rate ϕ by equation 2.

$$t = (T_0 - T) / \phi \quad \text{Equation 2}$$

The relative crystallinity $X(t)$ as a function of time t developed from equations 1 and 2 for HDPE and the HDPE/$CaCO_3$ composites are shown in Figure 2. The results show that the crystallization time reduced gradually with the increasing cooling rate. The half times $t_{1/2}$ for the non-isothermal crystallization can be obtained from Figure 2 and are presented in Table 1.

Non-isothermal crystallization kinetics

The time-dependent relative crystallinity function $X(t)$ for the non-isothermal crystallization process can be adopted from the Avrami equation (Xu *et al*., 2003; Xu *et al*., 2004) and are derived in equation 3:

$$X(t) = 1 - \exp(-Z_t t^n) \quad \text{Equation 3}$$

where:

Z_t is the Avrami rate constant involving the nucleation and growth parameter,

t is the crystallization time,

n is the Avrami exponent which depends on the nucleation and growth mechanism.

By rearranging equation 3 and taking the double logarithm, the following relation in equation 4 is obtained:

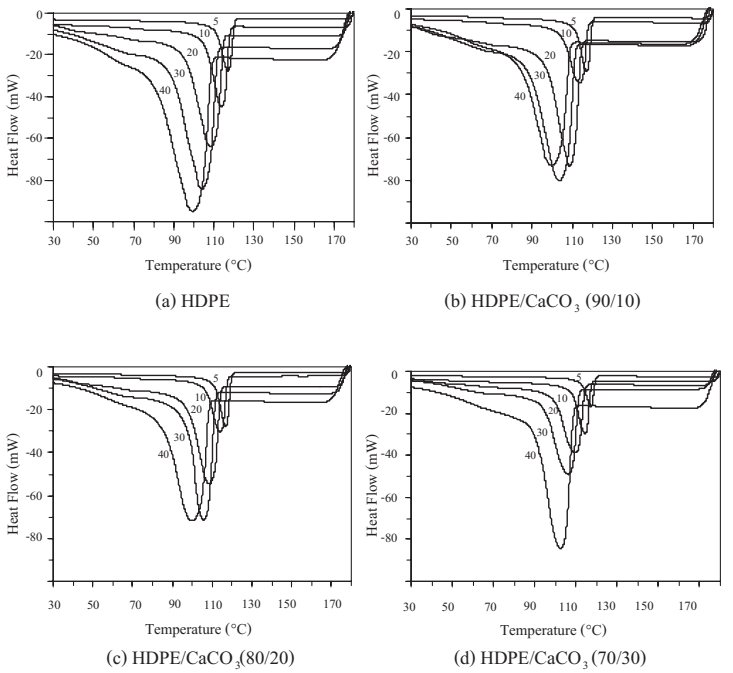

Figure 1 DSC curves of the non-isothermal crystallization of HDPE and the HDPE/$CaCO_3$ composites at 5, 10, 20, 30 and 40°C/min cooling rates.

Table 1 Non-isothermal parameters for HDPE and the HDPE/$CaCO_3$ composites determined from DSC exotherms.

HDPE:$CaCO_3$ (wt %)	ϕ (°C/min)	T_o (°C)	T_p (°C)	T_e (°C)	ΔH_c (J/g)	$t_{1/2}$ (min)	n	Z_c
100;0	5	120.2	117.3	111.3	138.5	1.29	3.00	1.25
	10	118.0	113.9	107.4	142.8	0.77	2.70	1.04
	20	114.8	108.5	97.6	150.1	0.57	2.70	1.06
	30	111.8	104.2	90.4	153.2	0.44	2.64	1.06
	40	108.9	99.7	80.1	154.3	0.39	2.44	1.05
90;10	5	120.0	117.2	112.2	136.0	1.31	3.30	1.29
	10	117.7	113.7	104.8	140.9	0.83	2.64	1.01
	20	114.4	108.6	96.6	142.3	0.50	2.48	1.07
	30	111.6	103.7	89.0	143.5	0.45	2.58	1.06
	40	108.9	99.7	88.5	144.0	0.35	2.42	1.06
80;20	5	119.6	116.0	111.0	118.3	1.22	3.17	1.22
	10	117.5	114.1	106.4	119.4	0.73	2.80	1.05
	20	114.2	108.5	97.5	124.3	0.51	2.57	1.07
	30	111.5	105.8	93.2	126.5	0.33	2.64	1.09
	40	108.5	99.9	85.2	127.7	0.32	2.23	1.05
70;30	5	119.4	117.4	112.3	91.2	1.06	3.44	1.12
	10	117.3	114.4	107.8	95.7	0.68	3.44	1.10
	20	114.2	109.7	99.4	104.3	0.45	2.67	1.09
	30	111.4	106.5	93.9	106.2	0.35	2.62	1.08
	40	108.5	102.7	89.9	111.8	0.27	2.50	1.08

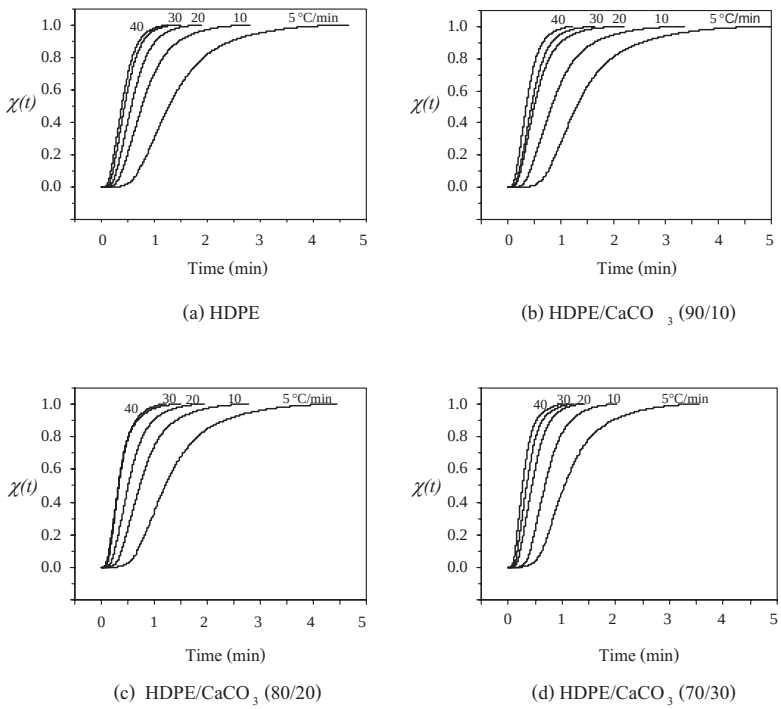

Figure 2 Plots of $\chi(t)$ versus t during the non-isothermal crystallization process for HDPE and the HDPE/$CaCO_3$ composites.

$$\log \{-\ln[1 - X(t)]\} = n \log t + \log Z_t \quad \text{Equation 4}$$

In the non-isothermal process, Jeziorny adopted the crystal growth rate constant Z_t in equation 4 by Z_c, using equation 5:

$$\log Z_c = \log Z_t / \phi \quad \text{Equation 5}$$

The Avrami plots of log{-ln[1-$X(t)$]} against log t (min) for each cooling rate are shown in Figure 3. The results show a straight line at $X(t)$ below 60%. The parameters n and Z_t can be evaluated from the slope and the intercept of the Avrami plot. The two parameters n and Z_c obtained from the Avrami plots and the Jeziorny method are also listed in Table 1.

For $X(t)$ below about 60%, the Avrami exponent n decreased with an increase in the cooling rate. At the 5°C/min cooling rate, the exponent n of HDPE was less than that of the HDPE/$CaCO_3$ composites. The crystal growth constant Z_c was nearly unchanged at a cooling rate of 10-40°C/min; but at a 5°C/min cooling rate, the value of Z_c dramatically increased. The value of n decreased from 3.0 to 2.4, and Z_c decreased from 1.2 to 1.0 for HDPE, while n decreased from 3.4 to 2.2 and Z_c decreased from 1.3 to 1.0 for the HDPE/$CaCO_3$ composites as the cooling rate increased from 5°C/min to 40°C/min.

Combined Avrami equation and Ozawa equation

In order to describe exactly the whole non-isothermal crystallization process, a method developed by Liu and co-workers was employed (Qiao *et al*., 2000; Joshi and Butola, 2004). The kinetic equation for the non-isothermal crystallization behavior for a given degree of crystallinity can be expressed by equation 6:

$$\log Z_t + n \log t = \log K(T) - m \log \phi \quad \text{Equation 6}$$

where:

$K(T)$ is a cooling function depending on the nucleation mechanism, nucleation rate and the

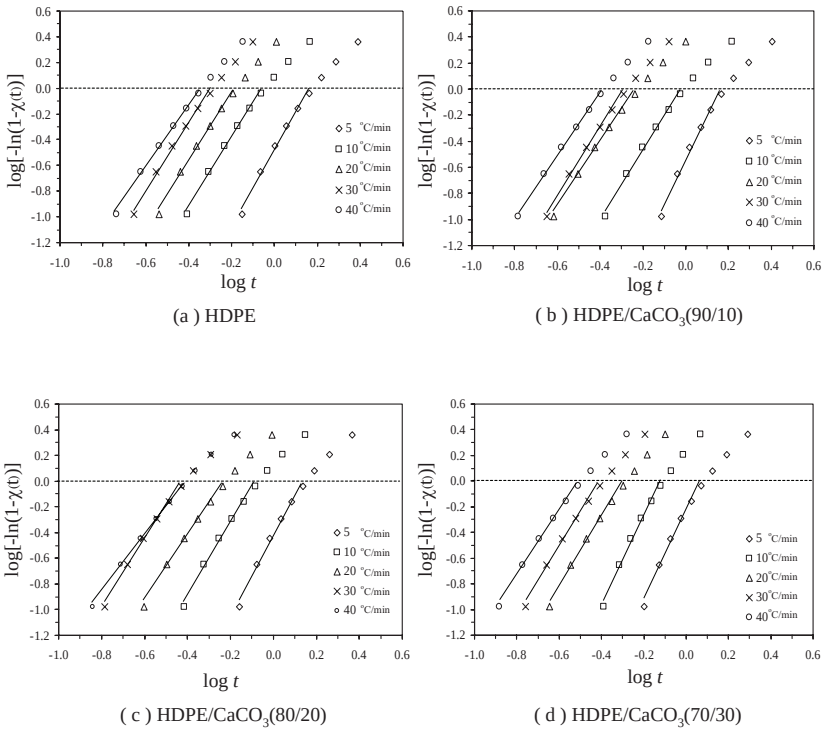

Figure 3 Plots of log{-ln[1-χ(t)]} versus log *t* during the non-isothermal crystallization process.

growth rate of the crystal,

m is the Ozawa exponent.

Rearranging equation 6 produces equation 7:

$$\log\phi = \log F(T) - a\log t \qquad \text{Equation 7}$$

where:

$F(T) = [K(T)/Z_t]^{1/m}$

the parameter F(T) refers to the cooling rate which is chosen at the unit crystallization time when the measured system reaches a certain degree of crystallinity,

$a = n/m$, is the ratio of the Avrami exponent *n* to the Ozawa exponent *m*.

A plot of log ϕ versus log *t* should give a straight line with an intercept of log *F(T)* and a slope of *a*. The plots of log ϕ versus log *t* for HDPE and the HDPE/$CaCO_3$ composites are presented in Figure 4 and show a near-linear relationship between log ϕ and log *t*. The values of *a* and *F(T)* listed in Table 2 indicate both *a* and *F(T)* increase uniformly with an increase in the relative degree of crystallinity. At a given relative crystallinity *X(t)*, the value of *a* decreases with an increase in the $CaCO_3$ content. The value of *F(T)* ranged from 2.70 to 14.71 for HDPE and from 2.87 to 14.78 for the HDPE/$CaCO_3$ composites. The crystallization rate increases as the value of *F(T)* decreases, indicating that the crystallization rate for HDPE and the HDPE/$CaCO_3$ composites was faster at the beginning and slowed down at the end of crystallization.

Crystallization activation energy

Kissinger described the crystallization activation energy ΔE of the non-isothermal crystallization process using equation 8:

$$\left\{ d\left[\ln(\phi / T_p^2) \right] \right\} / d(1/T_p) = -\Delta E / R \qquad \text{Equation 8}$$

where:

R is the gas constant,

T_p is the crystallization peak temperature.

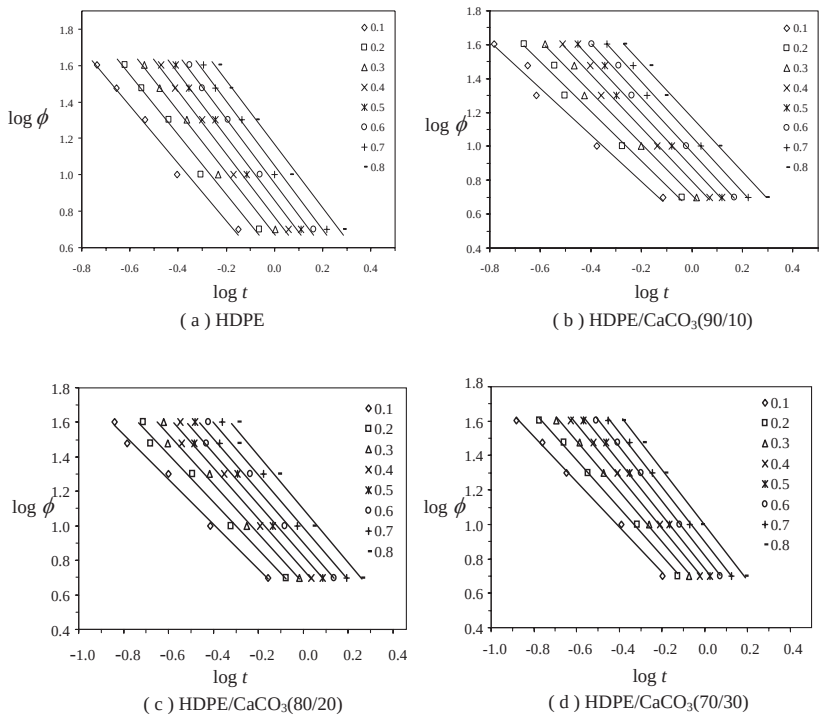

Figure 4 Plots of log ϕ as a function of log t for HDPE and the HDPE/$CaCO_3$ composites.

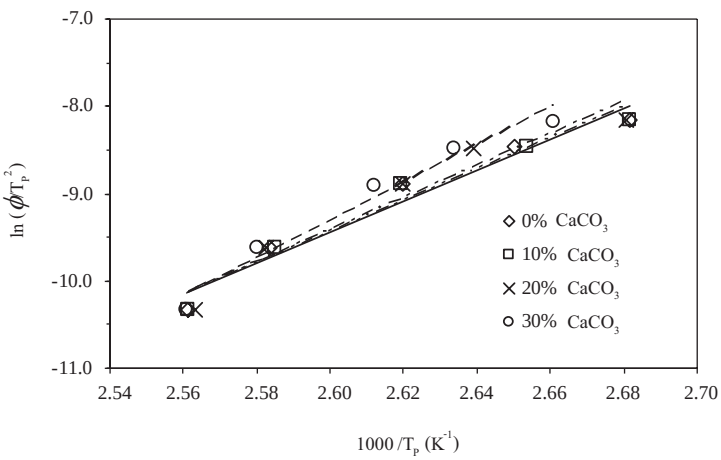

Figure 5 Plots of ln (ϕ/T_P^2) versus $1/T_p$ for HDPE and the HDPE/$CaCO_3$ composites.

Plots of ln (ϕ/T_p^2) against $(1/T_p)$ for HDPE and the HDPE/$CaCO_3$ composites are shown in Figure 5. The crystallization activation energy ΔE determined from the slope of the line is also listed in Table 2, which shows that the value of ΔE is nearly constant for HDPE and the HDPE/$CaCO_3$ composites up to 20% $CaCO_3$, but increases slightly for the 30% $CaCO_3$ system.

CONCLUSIONS

The non-isothermal crystallization

Table 2 Non-isothermal crystallization kinetic parameters for HDPE and the HDPE/$CaCO_3$ composites.

HDPE : $CaCO_3$	$\chi(t)$	a	$F(T)$	ΔE (kJ/mol)	HDPE : $CaCO_3$	$\chi(t)$	a	$F(T)$	ΔE (kJ/mol)
100:0	0.1	1.58	2.70	147.5	80:20	0.1	1.31	3.05	152.1
	0.2	1.65	3.64			0.2	1.38	3.83	
	0.3	1.70	4.67			0.3	1.44	4.64	
	0.4	1.73	5.84			0.4	1.47	5.61	
	0.5	1.75	7.23			0.5	1.49	6.67	
	0.6	1.76	8.96			0.6	1.51	7.99	
	0.7	1.77	11.29			0.7	1.52	9.73	
	0.8	1.74	14.71			0.8	1.55	12.48	
90:10	0.1	1.38	3.29	146.9	70:30	0.1	1.35	2.87	177.5
	0.2	1.46	4.18			0.2	1.40	3.44	
	0.3	1.52	5.14			0.3	1.46	4.03	
	0.4	1.57	6.25			0.4	1.51	4.71	
	0.5	1.60	7.56			0.5	1.55	5.53	
	0.6	1.62	9.20			0.6	1.58	6.55	
	0.7	1.63	11.39			0.7	1.60	7.88	
	0.8	1.61	14.78			0.8	1.61	9.91	

kinetics of HDPE and the HDPE/$CaCO_3$ composites (10, 20 and 30% wt, $CaCO_3$) were investigated using a differential scanning calorimetry (DSC) technique. The melt was cooled at 5 cooling rates: 5, 10, 20, 30 and 40°C/min. The Jeziorny model modified from the Avrami method was used for the investigation of non-isothermal crystallization. The results showed that for a relative degree of crystallinity of less than 60%, the Avrami exponent n decreased with an increase in the cooling rate. While the crystal growth constant Z_c, was nearly unchanged for both HDPE and the HDPE/$CaCO_3$ composites, at a 10-40°C/min cooling rate and at a cooling rate of 5° C/min, the value of Z_c dramatically increased. The value of Z_c decreased from 1.2 to 1.0 for HDPE and 1.3 to 1.0 for the HDPE/$CaCO_3$ composites as the cooling rate increased from 5°C/min to 40° C/min.

The combined Avrami-Ozawa model developed by Liu *et al*. was employed to describe the crystallization behavior of HDPE and the HDPE/$CaCO_3$ composites. The results showed that both a and $F(T)$ increased systematically with an increase in the relative crystallinity. At a given relative crystallinity, the value of a decreased with an increase in the $CaCO_3$ content, but the value of $F(T)$ was highest for 10% $CaCO_3$ and then decreased as the $CaCO_3$ content increased. Thus, the crystallization rate for HDPE/10% $CaCO_3$ was the slowest at a given cooling rate. The activation energy determined from the Kissinger method indicated little difference in the values of the activation energy for all systems, except the 30% $CaCO_3$ system which showed a slightly higher activation energy.

LITERATURE CITED

Fonseca, C. A. and I. R. Harrison. 1998. An investigation of co - crystallization in LDPE/ HDPE blends using DSC and TREF. **Thermochim. Acta.** 313: 37-41.

Joshi, M. and B.S. Butola. 2004. Studies on non-isothermal crystallization of HDPE/POSS nanocomposites. **Polym.** 45:4953-4968.

Krumme, A., A. Lehtinen and A. Viikna. 2004. Crystallization behavior of high density polyethylene blends with bimodal molar mass distribution, non-isothermal crystallization. **Eur. Polym. J.** 40: 371-378.

Mehta, N., D. Kumar and A. Kumar. 2004. Calorimetric studies of the crystallization growth process in glassy $Se_{70}Te_{30-x}Ag_x$ alloys. **Turk J. Phys.** 28: 397-406.

Qiao, X., X. Wang, X. Zhao, Z. Mo And H. Zhang. 2000. Non-isothermal Crystallization of poly (3-dodecylthiophene) and poly (3-octadecylthiophene). **Synth. Met**. 113: 1-6.

Salazar, D., J. S. Rodriguez, C. Albano and R. Sciamanna. 2002. Development and evaluation of an evolutionary tool for obtaining the crystallization rate constant of semicrystalline polymers (HDPE case) as a function of temperature. **Eu. Polym. J.** 38: 1001-1012.

Wang, H. L., T.J. Shi, S.Z. Yang and G.P. Hang. 2006. Crystallization behavior of PA6/SiO_2 organic-inorganic hybrid material. **Mater. Res. Bull.** 41: 298-306.

Xu, W., G. Liang, W. Wang, S. Tang, P. He and W.-P. Pan. 2003. Poly(propylene) - Poly(propylene) – Grafted Maleic Anhydride – Organic Montmorillonite (PP-PP-g-MAH-Org-MMT) Nanocomposites. **J. Appl. Polym. Sci.** 88: 3093-3099.

Xu, W., H.B. Zhai, H.Y. Guo, Z.F. Zhou, N. Whitely and W.P. Pan. 2004. PE/ORG-MMT nanocomposites no-isothermal crystallization kinetics. **J. Them. Anal. Cal.** 78: 101-112.

Zhang, C., H. F. Wu, C. A. Ma and M. Sumita. 2006. Effect of vapor grown carbon fiber on non-isothermal crystallization kinetics of HDPE/PMMA blend. **Mater. lett.** 60: 1054-1058.